Fast algorithm for the determination of the optimum filter for bone SPECT image reconstruction

Afef houimli (houimliafef13@gmail.com)
Université de Tunis El Manar
Issam benmhammed
Université de Tunis El Manar
Bechir letaief
Université de Tunis El Manar
Dorra Ben-Sellem
Université de Tunis El Manar, Institut Salah AZAIEZ

Research Article

Keywords: SPECT, bone SPECT image denoising, 3D FBP, Shepp Logan phantom

Posted Date: March 9th, 2021

DOI: https://doi.org/10.21203/rs.3.rs-304415/v1

Abstract

In SPECT, the reconstructed images are strongly affected by poisson noise, poor spatial resolution and bad contrast due to the radioactivity disintegration and procedures acquisition. In this paper, we propose an algorithm to improve the traditional FBP reconstruction and to choose the most suitable technique for bone SPECT image denoising. The proposed approach is composed of two steps. The first one consists of denoising the acquired sinograms using successively eight currently used filters in nuclear medicine: Wiener, Metz, Hamming, Hann, Shepp-Logan, Parzen, Butterworth and Gaussian combined with Butterworth filters. The second step is a simultaneous reconstruction of the axial slices using a new 3D FBP algorithm for each filter. A comparative study of these filters is tested and evaluated on a dataset containing thirty one bone SPECT image. The results show that the difference between these filters is statistically significantly different from each other ($p<0.05$) and the 3D FBP with the combination between Butterworth and Gaussian provide the best performance. The selected method is compared to three denoising methods. These methods are tested on a Shepp Logan phantom and bone SPECT images. Experimental results show that the 3D FBP reconstruction with the pre-processing combination (Gaussian (Std=0.3) + Butterworth (fc=0.47, ordre=3)) filter is more accurate and robust compared to other methods. It provides the highest performance in term of contrast, SNR, CNR ensuring a shorter processing time. It accelerates the reconstruction, reduces noise and artifacts while preserving detailed features. This approach could be considered as a valuable candidate to enhance the quality of the reconstructed bone SPECT image.

1. Introduction

Single photon emission computed tomography (SPECT) is a non invasive functional imaging modality which enables in vivo examination of organs' function. SPECT based on the administration to patients of a gamma emitter labeled radiopharmaceutical for diagnostic or therapeutic purpose. The head of detection of the gamma camera is mounted on a frame rotates around the patient to record multiple projections of the radioactive concentration under different angles of view. The projection images are stored on the computer where it will be recombined mathematically for reconstructing either sequences of tomographic slices in 3 directions. This technique allows the doctors to perform an accurate diagnostic of the radiopharmaceutical distribution in any slice of the body. Reconstructive methods are divided into two approaches: analytic and iterative methods. The analytic method, such as Filtered Back-Projection (FBP), is the standard reconstruction algorithm currently used in nuclear medicine tomography because of its facility and speed [1]. Versus the iterative method which requires a longer computational time. The analytic reconstruction method requires sufficient projection data with low noise. However, in practical experiment in nuclear medicine the number of projection sets is limited provoking streak artifacts, inducing more noise, masking same organs, reducing lesion detection and making the obtained images unreadable. To overcome these problems, the data must be filtered prior the back- projection [2]. For de-noising the reconstructed SPECT image, several studies of filtering have been investigated [3][4]. Many of them proved that the low-pass filters obscure the significance of small lesions, smoothen the details and reduce the sensitivity of the methods [5]. However, the restoration filters increase image contrast, improve lesion detection, amplify the artifacts at certain frequencies and reduce the specificity of the methods [6][7]. In [8], a comparison made between the FBP reconstruction with Butterworth pre-processing filter and OSEM iterative reconstruction. The previous work demonstrated that the FBP method with a Butterworth filter provides the optimal SPECT image quality. Furthermore, this method is more efficient

for standardizing the reconstruction parameter for the head and chest images, but these parameters were more operator-dependent for the abdomen. In [9], S. YU and al proposed a new approach for SPECT image denoising, called 'the patch confidence Gaussian filter (PCG)', and compared their performance to three methods: Pre and post denoising median filter and the pre- processing Gaussian filter followed by the Maximum Likelihood Expectation Maximization (MLEM) iterative reconstruction. they demonstrated that their method enhances efficiently the quality of SPECT image. In [10] M. T. Madsen and al show that the Gaussian filter enhance the contrast and suppress noise in the reconstructed bone SPECT slices.

On the other hand, there has been a significant conflict in the selection of the appropriate filter and adjustment of their parameters to individual cases [11][12]. In the literature, several studies have been proposed to choose the appropriate filter with the best parameters for each region and for each organ. In [13], Alirza S. and al applied the cosine, Hamming, Han, Shepp-Logan and Ram-Lak on the hot region of Carlson phantom SPECT image. They shown that Ram-Lak and Shepp-Logan filters with 0.4 cut-off frequencies improve the perceived image quality of hot region and their detectability.

S. Sayed et al. [14] applied a Butterworth filter of order 5 with cut-off frequencies 0.35 and 0.45 cycles•cm−1 on a cylindrical phantom filled with Tc-99m solution. They have demonstrated that the contrast and region's detectability were improved with the use of 0,45 cycles•cm−1 cut-off frequency.

To summarize, much research demonstrates that the FBP reconstruction, particularly the FBP based on both Gaussian filter and Butterworth filter, provide the best SPECT image quality. Other studies show that the major drawback of this approach is the severity and the

extend of the artifact, which makes the denoising process inaccurate and difficult near the hyper fixation activity. In this paper, we continue the research in this area, we use the previous studies results as a starting point and we research on the performance of eight pre-processing widely used filters in nuclear medicine with various parameters, followed by a proposed 3D FBP for improving the reconstruction of a dataset composed of Tc99m-HMDP bone SPECT images, taken from the radiology department of National Oncology Institute"Salah AZAIZE" of TUNIS. First, we investigate the performance and the capability of the following filters to reduce the artifact: Wiener and Metz filters as restoration filters and Hamming, Hann, Shepp-Logan, Parzen, and Butterworth filter as smoothing filters [4]. Then we propose a combination between the contrast enhancement Gaussian filter with the noise reducing Butterworth filter. For each filter various parameters are tested. After that, the pre- processing technique which provides the highest performance is compared to three methods: 3D FBP based on Gaussian filter, 3D FBP based on Butterworth filter and 2D FBP based on Gaussian combined with Butterworth filter. Furthermore, the quantitative values of the proposed method are compared to those of some previous study methods. The rest of this paper is structured as follows: section 2 describes the used methods, section 3 presents the obtained results and compares the used reconstruction methods, section 4 presents the discussion and in section 5 the paper concludes this work.

2. Materials And Methods

The method proposed to accelerate the reconstruction as well as improve the quality of reconstructed images includes two steps: pre-processing step using different filtering conditions and a reconstruction step based on a ramp 3D Back Projection implementation. Fig 1. Shows the block diagram of the proposed algorithm.

In the following, we will present our approach in details by focusing on the following steps.

2.1. Sinogram images denoising:

The acquired tomosintigraphic projection images suffer from bad resolution and fluctuations due to the Poisson distribution [15]. In order to choose the optimum filter for bone SPECT image that reduces efficiently the noise as much as possible preserving the image details, we applied eight widely used filters in nuclear medicine, in frequency domain, as shown in fig2, which is used in[10] for one filter:

FILTRATION: To cover the whole range of variables, a total of 137 filtering conditions were considered as shown in TABLE1.

Table 1:. Filtering conditions

Butterworth	fc	0.1	0.15	0.2	0.23	0.27	0.3	0.35	0.4	0.45	0.5	0.6	0.7	0.8
	order	2			3			5		7		9		
Metz	order	7.8												
	MTF	3.5												
Wiener	FWHM	7.8												
	SNR	11												
Hanning, Hamming, Shepp-Logan Parzen, gaussian	cf	0.15	0.2	0.23	0.27	0.3	0.35	0.4	0.45	0.5	0.6	0.7	0.8	0.9
Butterworth+ Gaussian	cf	0.15		0.2		0.25		0.3		0.35		0.4		0.47
	order	2		3				5				9		
	standard deviation	0.15		0.2		0.25		0.3			0.4		0.5	

2.2. Modified 3D Back projection Reconstruction.

The 2D Back projection reconstruction using ramp filter assures the retro-projection of one image. So, the reconstruction of a 3D image requires a longer time. To accelerate the reconstruction step, we propose a 3D Back projection based on ramp filter, where we convert the input sequence of sinogram images to a 3D matrix, then we apply the 3D Back projection presented in fig3. Therefore, a 3D axial slice image is reconstructed simultaneously and not successively in the interactive calculation, contrariwise to the 2D Back projection reconstruction (slice-by-slice).

2.3.Optimization of the proposed method for bone SPECT image reconstruction:

To select the optimum filter for bone SPECT image reconstruction, We analyzed eighty anonymous bone SPECT images taken from the radiology department of National Oncology Institute ”Salah AZAIZE” of TUNIS, generated by a double-head gamma camera- CT model with a parallel collimator, equipped with a low dose CT scan characterized by a low energy and ultra-high-resolution characteristics. All patients are injected standard doses according to EANM guidelines. The bone scan tomographies are performed according to protocols (32 projections per head and twenty seconds per projection). The protocols are standardized for all patients. This dataset acquired during the period from the 6th July 2015 to the 29th June 2016 for diagnosis of metastasis in oncology patients. We chose thirty one (31) studies with a significant abnormal increased uptake on bone

scan, 9 males and 21females aged between 45 and 75 years. Each DICOM image is a sequence of 128 projections (720°) as shown in fig4 and a 128*128 matrix with a pixel spacing equal to 4.795 mm. After reconstruction, we calculated some criteria including mean contrast, mean signal to noise ratio (SNR) and mean contrast to noise ratio (CNR) of all the slices containing the lesion for each exam as follows:

Two experts in nuclear medicine draw the ROIs through the hyperfuctionning bone locations from the normal bone to abnormal region and further in the transverse views of bone image, using MATLAB (R2013a) environment as shown in Fig. 5. These regions are the same for all the filtered slices that contain the lesion for each exam (in our case, the number of slice for each exam didn't exceed 13 slices).

For each patient and for each filter, the number of SPECT transverse slices containing bone lesions multiplied by the total number of combinations (305 combinations) was analysed. We measured the maximum count in normal bone, maximum count in hyperfuctionning bone and minimum count in the background for each slice. Then, by using all of these measurements, we calculated the contrast, signal to noise ratio (SNR) and Contrast-to-noise Ratio (CNR) as follows:

Contrast = (N max (abnormal) - N max (Normal)) / N max(Normal) (1)

SNR = (Nmin(abnormal) -Nmax(Normal))/ Nmin(background) (2)

CNR =(Nmax(abnormal) -Nmax(Normal))/s (3)

Where Nmax(Normal) is the maximum count in normal bone, Nmax(abnormal) is the maximum count in hyperfuctionning bone, Nmin(background) is the minimum count in the background and σ is the standard deviation in the background.

Quantitatively, the optimum filter has the highest value of contrast, CNR and SNR. So, the first purpose of this work is to select the best combination of parameters for each filter. The second purpose is to choose the best filter. We evaluate the performance of each combination of filter parameters. In fact, the combination of filter parameters that provides the highest CNR, SNR and contrast as the most suitable for bone SPECT image de-noising. Numerical results on all the patients' data revealed that maximum contrast, CNR and SNR could be obtained using the Butterworth (cutoff 0.2-0.7, order 3-9), Hanning (cutoff 0.15 - 0.5), Hamming (cutoff 0.15 - 0.5), Shepp-Logan (cutoff 0.23-0.48),Parzen(cutoff 0.15-0.5), Metz (order=9.5,FWHM=7.8mm), Wiener (order=9.5,SNR=11) and Butterworth(cutoff=0.47,order=3) combined with Gaussian (Std=0.3), that's why we use the statistical Analysis. We performed Jarque-Bera test for testing whether the series were normally distributed, this test is based on the sample skewness and sample kurtosis.The asymmetry coefficient (coefficient of skewness) is near 0 for most values. As for the kurtosis (kurtosis coefficient), we noted that all distributions had a coefficient greater than 3, so they are leptokurtic (the presence of fat tails). From the point of view of statistics Jarque-Bera normality, assumption can accept some values during our study.

Performing One-Way ANOVA-test, significant difference ($P<0.05$) was observed between contrasts, SNR and CNR generated by Butterworth, Hamming, Hann, Shepp-Logan, Parzen, Metz, Wiener and Butterworth combined with Gaussian filters as shown in Table1 ,2 and 3.

Table 2: Comparison of filters in mean contrasts for eight filters

Filter	N	Mean contrast	df	F	*Sig*
Butterworth (cutoff=0.2,order=7)	31	6.90	Between groups = 447 Within Groups = 1952 Total = 2399	1.554	0.00
Butterworth(cutoff=0.5, order=3)	31	6.85			
Butterworth(cutoff=0.57, order=5)	31	6.80			
Butterworth(cutoff=0.2, order=9)	31	5.54			
Hamming(cutoff=0.27)	31	5.43			
Hann(cutoff=0.3)	31	6.00			
Shepp-Logan(cutoff=0.15)	31	5.81			
Parzen(cutoff=0.2)	31	6,00			
Metz(order=9.5, FWHM=7.8mm)	31	1.3524			
Wiener(order=9.5, SNR=11)	31	1.2659			
Butterworth(cutoff=0.47,order=3)+Gaussian (Std=0.3)	31	6.96			

Table 3: Comparison of filters in mean SNRs for eight filters

Filter	N	Mean SNR(db)	df	F	Sig
Butterworth(cutoff=0.2, order=7)	31	60.32	Between Groups = 7 Within Groups = 278 Total = 285	2.61	0.013
Butterworth(cutoff=0.5, order=3)	31	61.05			
Butterworth(cutoff=0.57,order=5)	31	60.50			
Butterworth(cutoff=0.2, order=9)	31	61.54			
Hamming(cutoff=0.27)	31	60.63			
Hann(cutoff=0.3)	31	58.06			
Shepp-Logan(cutoff=0.15)	31	56.61			
Parzen(cutoff=0.2)	31	58.60			
Metz(order=9.5,FWHM=7.8mm)	31	54.13			
Wiener(order=9.5, SNR=11)	31	33.06			
Butterworth(cutoff=0.47,order=3)+Gaussian(Std=0.3)	31	61.02			

Table 4: Comparison of filters in mean CNRs for eight filters

Filter	N	Mean CNR(db)	df	F	*Sig*
Butterworth (cutoff=0.2, order=7)	3150.58		Between Groups= 10	1.529	0.000
Butterworth (cutoff=0.5, order=3)	3158.48		Within Groups= 330		
Butterworth (cutoff=0.57, order=5)	3157.80		Total = 340		
Butterworth(cutoff=0.2, order=9)	3157.86				
Hamming (cutoff=0.27)	3141.43				
Hann (cutoff=0.3)	3141.96				
Shepp-logan (cutoff=0.15)	3125.81				
Parzen (cutoff=0.2)	3115,00				
Metz(order=9.5,FWHM=7.8mm)	3141.35				
Wiener(order=9.5, SNR=11)	3121.26				
Butterworth(cutoff=0.47,order=3)+ Gaussian (Std=0.3)	3160.96				

Quantitavely Table 1, Table2 and Table3 summarizes the mean contrast, the mean SNRs and the mean CNRs calculated from SPECT axial slices with different combination of filter parameters(305*nombre of SPECT transverse slices containing lesion).

These results showed that these performances are the lowest for Metz and Wiener, best for the smoothing filters as Hamming, Hanning, Shepp-Logan, Parzen and Butterworth.

Gaussian (Std=0.3) combined with Butterworth (cutoff=0.47, order=3) filters provide the maximum performance in the group.

Qualitatively, Fig 6 shows that:

The smoothing filters had a quite similar effect on image quality; these filters attenuate the details and the shape of the image. The streaking artifacts persisted in the filtered image.

Metz and Wiener filters have characteristics of both the smoothing and blurring compensation. The Wiener filter is a linear filter widely used to reduce the noise in scintigraphic images. The aim of this filter is to find an image with a minimum mean squared error between the original image and the restored image. The smoothing power of Metz filter increases as the system spread function flattens. In our study, these filters provides blurred image with streaking artifacts.

Butterworth filter combined with Gaussian provides the best quality of image; this combination reduces the streaking artifacts with the best degree of accuracy and minimal degradation of the boundaries of the regions and the small detail.

Clinical sensitivity and specificity evaluation:

Two expert radiologists evaluated the filtered slices by the proposed method. The possible outcomes of this evaluation were calculated as follows: true positive=10, true negative=1, false positive=2 and false

negative=17. From these values, the corresponding sensitivity= 90, 9 %, Specificity=89, 5 %, positive predictive value (PPV) =83,3%, negative predictive value (NPV) =94,4% and accuracy=90%. This results show that the proposed method was able to provide potentially useful information for the interpretation of bone SPECT images. Furthermore, the clinical sensitivity and specificity diagnosis in Bone SPECT images rise if SNR and Contrast increase.

Results

In this section, we present a description of the phantom and bone SPECT database obtained from radiology department of National Oncology Institute ”Salah AZAIZE” of TUNIS. Then we present the different results and performance analysis of the proposed method.

1. database description:

(a) Three-dimensional Shepp–Logan phantom

To evaluate the methods in term of robustness of reconstruction and image quality, we tested the different algorithms on a 3D Shepp-Logan phantom. The distribution of projection data assumed to be generated by 128 angular views (distributed in the range of 180 degrees).

For simulation study of the different reconstruction methods, we added the Poisson noise to the projection data. Then, we tested various parameters to select the best one for each method.

The performance of the different method was evaluated from the following objective criteria:

$$\text{Contrast} = \left| \frac{\mu_s - \mu_b}{\mu_b} \right| \quad (3)$$

$$\text{Noise} = \frac{\sigma}{\mu_b} (4)$$

$$\text{CNR} = \frac{\text{Contrast}}{\text{Noise}} (5)$$

Where μ_s is the mean activity of lesion S, σ and μ_b represent respectively the standard deviation and the mean activity in a background region.

Patients studies

For each method, we calculated the value of SNR defined in equation (1), the contrast defined in equation (2) and the time of execution for 31 bone SPECT exam.

2. Shepp–Logan phantom Result:

To illustrate the phases presented in Section 2, Fig. 11 shows the different results of the proposed method at gray level images. Column (A) depicts the original phantom image, column (B) presents the original projection,

column(C) presents the noisy projection, column (D) presents the noisy sinogram, column (E) presents the filtered sinogram and column (F) shows the reconstructed phantom image.

3. data results:

In this part, we present the reconstructed slice images at three standard planes of the bone SPECT image presented in Fig.4. The sequence of transversal, coronal and sagittal slices of bone images filtered by the best Filter (Butterworth (cutoff=0.47, order=3)+Gaussian (Std=0.3)) are presente in Fig.11, Fig12 and Fig.13

2.4. Performance evaluation:

To evaluate the performance of the proposed method, we compared qualitatively and quantitatively the capability of our proposed method to 3D FBP based on Butterworth filter, 3D FBP based on Gaussian filter and 2D FBP based on Gaussian filter combined with Butterworth. First, a comparison is made between different performances for different parameters for the same technique, then a comparison is performed between the four methods with best parameters.

B. The filtering methods:

To obtain the best parameters of each algorithm; we applied the different method with different combinations of parameters on the sequence of sinograms as listed in table4. In the case of 3d FBP, the sequence of filtered sinograms were converted to 3 dimensional matrix, and back projected simultaneously by the proposed 3D back-projection. Whereas, in the case of 2D FBP, the sequence of filtered sinograms were successively back-projected by a direct inversion of the radon transform. Then, we quantified the resulted transverse slices (we choose one slice contain the lesion for each exam).

3D FBP based on Gaussian filter: The sequence of sonograms multiplied successively by the Gaussian filter. Table5 lists the different standard deviations used. We tested and compared the performance of each one. The obtained results shows that the Gaussian filter with (std= 0.4) provide the highest performance.

3D FBP based on Butterworth filter: The sequence of sinograms multiplied successively by the Butterworth filter. We tested the different parameters and we compared the performance of the resulted slices. The obtained results show that the Butterworth filter with (fc= 0.57 and =9) provide the highest performance.

3D FBP based on Gaussian filter combined with Butterworth filter: We tested the different combinations as listed in Table 5 for 3D FBP based on Gaussian combined with Butterworth filter and compared the performance of the resulted slice, the obtained results show that the Butterworth filter (fc=0.47 and order=3) combined with Gaussian filter (STD=0.3)) provide the highest performance.

2D FBP based on Gaussian filter combined with Butterworth.

We tested the different combinations as listed in Table 5 for 2D FBP based on Gaussian combined with Butterworth filter. Then we compared the performance of each resulted slice. The obtained results show that the Butterworth filter (fc=0.47, order=3) combined with Gaussian filter (std= 0.3) provides the highest performance.

Table 5: different combinations used in this study

Method	Fc	Order	std
2D and 3D FBP based on Gaussian filter combined with Butterworth filter	0.15, 0.2, 0.25, 0.3, 0.35, 0.4, 0.5	2	0.15, 0.2, 0.25, 0.3, 0.4, 0.5
	0.15, 0.2, 0.25, 0.3, 0.35, 0.4, 0.5	3	
	0.15, 0.2, 0.25, 0.3, 0.35, 0.4, 0.5	5	
	0.15, 0.2, 0.25, 0.3, 0.35, 0.4, 0.5	9	
3D FBP based on Butterworth filter	0.15, 0.2, 0.25, 0.3, 0.35, 0.4, 0.5	2	
	0.15, 0.2, 0.25, 0.3, 0.35, 0.4, 0.5	3	
	0.15, 0.2, 0.25, 0.3, 0.35, 0.4, 0.5	5	
	0.15, 0.2, 0.25, 0.3, 0.35, 0.4, 0.5	9	
3D FBP based on Gaussian filter			0.15, 0.2,0.25 0.3,0.4, 0.5

The reconstructed Shepp-Logan image obtained from various algorithms (2D FBP based on Gaussian combined with Butterworth filter (std=0.3, order=8, fc=4.8), 2D FBP based on Gaussian filter combined with Butterworth filter (std=0.3, order=9, fc=4.8), 3D FBP based on Gaussian filter (std=0.3) and 3D FBP based on Butterworth filter (fc= 0.57 and n=9)) are present in fig12.

Fig 13 illustrates the same profile of the corresponding Shepp-Logan image of one slice for the different reconstructed methods.

We present the values of performance of each method applied on the Shepp-Logan phantom image in Table6.

Table 6: CNR and reconstruction time of the Shepp-Logan phantom image

Reconstruction Method	Contrast	Noise	CNR	Reconstruction Time (sec)
3D FBP based on Gaussian filter combined with Butterworth filter	**0.7387**	**0.01**	**73.87**	68.57
3D FBP based on Butterworth filter	0,05691	0,011	5,69	65.64
3D FBP based on Gaussian filter	0,05806	0,011	5.27	65.94
2D FBP based on Gaussian filter combined with Butterworth filter.	0,5514	0,011	50,12	102.94

The tomo graphic bone SPECT slices reconstructed by the four methods with best parameters are present in Fig14.

Table 7: Comparison of the performance of the denoising methods applied on image presented in Fig.4

Method	Contrast	SNR(db)	Execution Time(sec)
SNR(dB)			
3D FBP based on Gaussian filter combined with Butterworth filter	**1,1380**	**85**	**5.140287**
3D FBP based on Butterworth filter	1,0563	69	6.814485
3D FBP based on Gaussian filter	1,0526	71	6.778485
2D FBP based on Gaussian filter combined with Butterworth.	1,1379	79	9.140287

For each method we calculated the mean value of contrast, SNR and time of execution for 31 bone SPECT exam as described in equations 1 and 2. Table 8, 9 and 10 shows the highlight of our contribution in term of contrast, SNR and processing time for 31 exams.

Table 8: Comparison between the reconstruction methods in mean Contrast

Method	N	Mean Contrast(dB)	ddl	F	Sig
2D FBP based on Gaussian combined with Butterworth filter	31	0,5348	Between Groups=3 Within groups =120 Total =123	1. 03,47	0,00
3D FBP based on Gaussian filter	31	0,4113			
3D FBP based on Butterworth filter	31	0,5287			
Proposed method	31	0,7555			

Table 9: Comparison between the reconstruction methods in mean SNR

Method	N	Mean SNR	ddl	F	Sig
2D FBP based on Gaussian combined with Butterworth filter	31	61.1935	Between Groups=3 WithinGroups=120 Total =123	19,302	0.00
3D FBP based on Gaussian filter	31	55,4839			
3D FBP based on Butterworth filter	31	48,2503			
Proposed method	31	63,5161			

Table10: Comparison between the reconstruction methods in mean execution time

Method	N	Mean execution time	ddl	F	Sig
2DFBP based on Gaussian combined with Butterworth filter	31	8.405	Between Groups= 3 Within Groups =120 Total =123	2,416	0.02
3DFBP based on Gaussian filter	31	6.245			
3DFBP based on Butterworth filter	31	6.2048			
Proposed method	31	**5.6439**			

2. Comparison with literature review work:

In [13], Secong et al. developed a de-noising technique labeled the Patch Confidence Gaussian (PCG), for SPECT image denoising, and compared their approach with two filters. Both filters combined with the Maximum Likelihood Expectation Maximization (MLEM) reconstruction algorithm. The auteur evaluated their approach on two myocardial axial slices using the signal to noise ratio defined as follows:

$$SNR = 20\log_{10}\frac{Y}{X}$$

Where Y and X are respectively the standard deviation of the count value of the object of interest region (ROI) and the mean counts value inside the same region.We implemented the Patch Confidence Gaussian (PCG) algorithm and we applied this technique on our bone SPECT images. Table 13 lists the SNRs values using the Secong methods and our methods.

Table11: Comparaison of SNR using the Secong method and our method

		Sincong method			Proposed method	
		Myocarde image	Bone image		Bone image	
		SNR (dB)	SNR (dB)	Time (sec)	SNR(dB)	Time(sec)
Unprocessing(ref)		17.8	16.3	224.43	**71**	**5.04**
reprocessing technique	Median filter	25.4	25.9	207.92		
	Gaussian filter	30.8	35.7	210.81		
	Gaussian+ butterworth		40.9	202.59		
	PCG filter	31.4	38.9	232.10		
stprocessing technique	Median filter	21.4	25.1	208.83		

We noticed that the Gaussian with Butterworth pre-filtering combined with MLEM reconstruction provide the highest performance in term of SNR and time of execution. In fact, the back projection filtering (FBP) provide a high value of SNR in a shorter time of execution compared to the iterative technique MLEM. We can conclude that FBP using the preprocessing combination (Gaussian+Butterworth) is better than the other technique for bone SPECT denoising.

As shown in Figure 15 and Figure 16, we develop a user graphical interface to facilitate the manipulation and display the desired slices according to the choice of the user. In first interface, the user can display the selected original projection and the filtered one filtered by a chosen filter. In second interface, the user can display, slice by slice or in montage, the slices according to the chosen filter and their parameters.

Discussion

In this paper, we proposed a novel 3D FBP reconstruction algorithm with eight currently used filters in nuclear medicine. This method presents a novel solution that allows the doctors to apply these filters successively on all the exams and reconstruct the slices in a shorter time than the conventional direct inversion of the radon transform. The main concern of this paper was to find the best filter, based on FPB method of reconstruction, which improve the bone SPECT image quality and reduce efficiently the generated streaking artifacts. This study shows that the 3D FBP reconstruction based on the contrast enhancement Gaussian (Std=0.3) combined with the noise reducing Butterworth (cutoff=0.47, order=3) method outperformed the other methods in terms of SNR, resolution and contrast, gain in reconstruction time, best reduction of artifacts and improved lesion detection of bone SPECT images reconstruction. To validate qualitatively and quantitatively the efficiency of our proposed algorithm, we compared in first step, the used pre–reconstruction filter with seven other filters. For a qualitative assessment, the filtered bone slices obtained from cited filters are illustrated in figure6. These results agree with I.Gunes and al [15] studies which showed that the Butterworth filter return the

more efficiency anatomic details than other filters. In contrast to some reports in the literature, we found that Metz and Shepp-Logan filters provide the worst image quality in term of resolution and contrast. In addition, these filters return images tainted both by a pixelization effect and by a smoothing.

We observe that the combination between Gaussian filter and Butterworth filter provide the best image quality in terms of noise and streaking artifacts reduction and preservation of the small details and the limit of region. Unlike the hanning, Hamming, Parzen and wiener filters which degrade the image quality by smoothing transitions and attenuating details which making delicate the extraction and the location of the contours. Indeed, the results of these filters contain a more artifacts in the form of oscillations which can be visually unpleasant. For quantitative assessment, the means SNRs, the means CNRs and the means contrasts are computed for each method. Table 1 shows that the means contrast of our proposed method is significantly superior to the other filter, this is explained by the efficiency of our proposed method to reduce the noisy artifact. Table 2 demonstrates that the proposed algorithm provides the highest means SNR values compared with the other filters which means that the coupling between Gaussian and Butterworth pre-reconstruction filtering succeeds to compromise between the poison noise reducing and the signal detail preservation.

Table3 shows that the proposed algorithm provides the highest means CNR values compared with the other filters which means that the combination between Gaussian and Butterworth pre-reconstruction filtering succeeds to reduce the noisy artifacts.

In second step, a comparison was made between the proposed technique and the 3D FBP based on Gaussian filter method and a 2D FBP based on Gaussian with Butterworth filter method both applied on a Shepp-Logan phantom image and a bone SPECT database.

For a qualitative assessment, figure12 represent the reconstructed Shepp-Logan images obtained from noisy projection using different method of reconstruction. This figure indicates that the proposed method allows the preservation of the original structure during the reconstruction by removing noise and conserving contrast. In fact, we can see that the reconstructed Shepp-Logan phantom image with the proposed method is the most similar to the original one.

Figure 14 shows that the 3D FBP based on Gaussian combined with Butterworth filter provides an improvement in the spatial resolution of the bone SPECT image. In fact, unlike the conventional 2D FBP where the slices are reconstructed successively in the interactive computation, the 3D FBP uses the full information content of the reconstruction volume which provides an accurate reconstruction of the distribution of the activity on the slice. Compared with our proposed technique, the 3D FBP based on the Gaussian filter method appears much noisy, which attenuate the detail by giving a blur effect on the edges and making delicate the extraction and the location of the contours. However, our proposed technique ensures good poison noise suppression with an accuracy preservation of the limit of region.

Quantitatively, Table5 shows the CNR and the reconstruction time of the different reconstruction methods applied on a Shepp-Logan phantom image. The value of these metrics favored the proposed method which demonstrates the efficiency of our proposed algorithm in reduction of noisy artefacts. Furthermore, table 5 shows that the proposed approach requires a shorter time of execution compared to other methods.

Fig 13 illustrates the same profile of the corresponding Shepp-Logan image of one slice for the different reconstruction methods. The result shows that the profile resulting from the proposed method is closer to the original profile than the other methods, which demonstrate the better preserves of the edges by removing noise, conserving contrast, while smoothing the region. Table 6 presents a comparison between the performances of the three denoising methods applied on the bone SPECT image presented in Fig.4. It is clear that the proposed method provides the highest performance.

Indeed, it is clear from Tables 7, 8, 9 and 10 that the SNR, the CNR and the contrast of our proposed method, tested on another 30 bone SPECT exam, is significantly higher than those in 2D FBP based on Gaussian with Butterworth filter, 3D FBP based on Gaussian and 3D FBP based on Butterworth for all the patient groups, which demonstrates the efficiency of our proposed algorithm in preservation of resolution and contrast, reduction of noisy artifacts and accuracy detection of lesion.

From Tables 11 and 12, we note that the processing time of our proposed approach is lower than the 2D FBP based on Gaussian combined with Butterworth filter due to the simultaneous reconstruction of slices. The 3D FBP based on Gaussian requires also a shorter time for processing, but still longer than our approach. To conclude, we can confirm that the proposed method achieve better result than the other methods in the enhancement of the quality of bone SPECT image reconstruction.

Conclusion

Filtered back projection reconstruction is the most currently used in nuclear medicine tomography and remains the standard for all the reconstruction algorithms. The aim of this paper was to choose the best de-noising filter for the tomography bone SPECT image reconstruction. Firstly, we applied a novel 3D FBP reconstruction algorithm with eight preprocessing filters on a dataset containing thirty one bone SPECT exams. Then, we evaluated their performance on the transverse slices. From the qualitative and quantitative comparative study that has been carried out, the 3D FBP based on Gaussian combined with Butterworth filter is the most efficient denoising method which can provide a notable gain in term of contrast, SNR, CNR and time of computation. Moreover, it can remove the noise from images with the best degree of accuracy and reduce the artifact without degradation of the contours and the small detail. Finally, it is possible to conclude that this approach is applicable to improve the quality of bone SPECT images reconstruction. In our future research we intend to concentrate on the preprocessing step of the proposed technique, more tests will be needed to enhance the quality of the tomography bone SPECT image reconstruction and devoid completely of artifacts.

Key Points

QUESTION: Any filter in nuclear medicine is the optimal for image reconstruction for Bone SPECT imaging?

PERTINENT FINDINGS: In a cohort study comparing the quality of the reconstructed image, for bone SPECT imaging, filtered by eight currently used filters in nuclear medicine. Each filter combined with a proposed fast reconstruction algorithm is tested and evaluated on a dataset containing thirty one bone SPECT image. The results show that the difference between these filters is statistically significant different from each other ($p<0.05$) and the 3D FBP with the combination between Butterworth and Gaussian provide the best

performance in term of noise and artifacts reduction, with detailed features preservation and gain of reconstruction time.

IMPLICATIONS FOR PATIENT CARE: The streaking artifacts generated with the FBP reconstruction is reduced using the proposed method, more tests will be needed to enhance the quality of the tomography reconstruction and devoid completely the artifacts in bone SPECT imaging.

References

[1] A. Sadremomtaz, P. Taherparvar, The influence of filters on the SPECT image of Carlson phantom, J. Biomedical Science and Engineering, 6(3)(2013)291-297 http://dx.doi.org/10.4236/jbise.2013.63037

[2] A. Sadremomtaz , P. Taherparvar, Quantitative and Qualitative Evaluations of Defect Images in Different Regions of Myocardial Phantom under Implementation of Various Filters in SPECT, Indian Journal of Science and Technology. 8 (12) (2015) DOI:10.17485/ijst/ 2015/v8i12/31943

[3]Gunes, I. Sarikaya, T. Ozkan, and T. Akbunar, Detection efficiency of different bone SPECT processing protocols for the diagnosis of “spina bifida”, Journal of Nuclear Biology and Medicine, 37(2)(1993) 49–52 https://www.ncbi.nlm.nih.gov/pubmed/8373832

[4] Lyra , A. Ploussi, Filtering in SPECT Image Reconstruction, International Journal of Biomedical Imaging 2011, 1–14. Article ID 693795 https://www.hindawi.com/journals/ijbi/2011/693795/

[5] M. Wheat, G.M.Currie, A Comparison of strategies for summing gated myocardial perfusion SPECT: are false negatives a potential problem?, Internet J Cardiol, 4(1) (2007)1-26, https://researchoutput.csu.edu.au/en/publications/a-comparison-of-strategies-for-summing-gated-myocardial-perfusion

[6] A. King, D.T.Long, B.A. Brill, SPECT volume quantitation: Influence of spatial resolution, source size and shape, and voxel size, Med Phys, 18(5)(1991): 1016-24.

[7] E. Fakhri, I. Buvat, H.T. Benali,R.D. Paola, Relative impact of scatter, collimator response, attenuation, and finite spatial resolution corrections in cardiac SPECT, J Nucl Med., 41(8) (2000)1400-8. https://www.ncbi.nlm.nih.gov/pubmed/10945534

[8] Massaro, S. Cittadin, F. Rossi, L. Rampin, E.Banti, O. Nibale, and D.Rubello, Reconstruction Parameters for 111In-Pentetreotide SPECT: Variability with Respect to Body Weight and Body Region” Journal of nuclear medicine technology, 35(4) (2007) :237-41 https://www.ncbi.nlm.nih.gov/pubmed/18006596

[9] S. YU, H.H.Muhammad, Denoising of SPECT-Image Sinogram-Data before Reconstruction, 18th World Multi-Conference on Systemics, Cybernetics and Informatics, Proceedings,1(2014) 202-206.

[10] T.Madsen and C. H. Park, Enhancement of SPECT Images by Fourier Filtering the Projection Image Set, J NuclMed 26(4)(1985) 395-402. / https://www.ncbi.nlm.nih.gov/ pubmed/3156976

[11] Taylor, Filter choice for reconstruct tomography. Nucl Med Commun 15(11) (1994) 857-9 https://www.ncbi.nlm.nih.gov/pubmed/7870390

[12] Rajabi, G.S.Pant, Optimum filtration for time-activity curves in nuclear medicine, Nucl Med Commun. 21(9) (2000):823-8. https://www.ncbi.nlm.nih.gov/pubmed/11065155

[13] Inayatullah S. S., Nor Syahirah M. N. " Effect of Cut-Off Frequency of Butterworth Filter on Detectability and Contrast of Hot and Cold Regions in Tc-99m SPECT" International Journal of Medical Physics, Clinical Engineering and Radiation Oncology 5(1)(2016) 100-109 http://www.malrep.uum.edu.my/rep/Record/my.iium.irep.49979

Figures

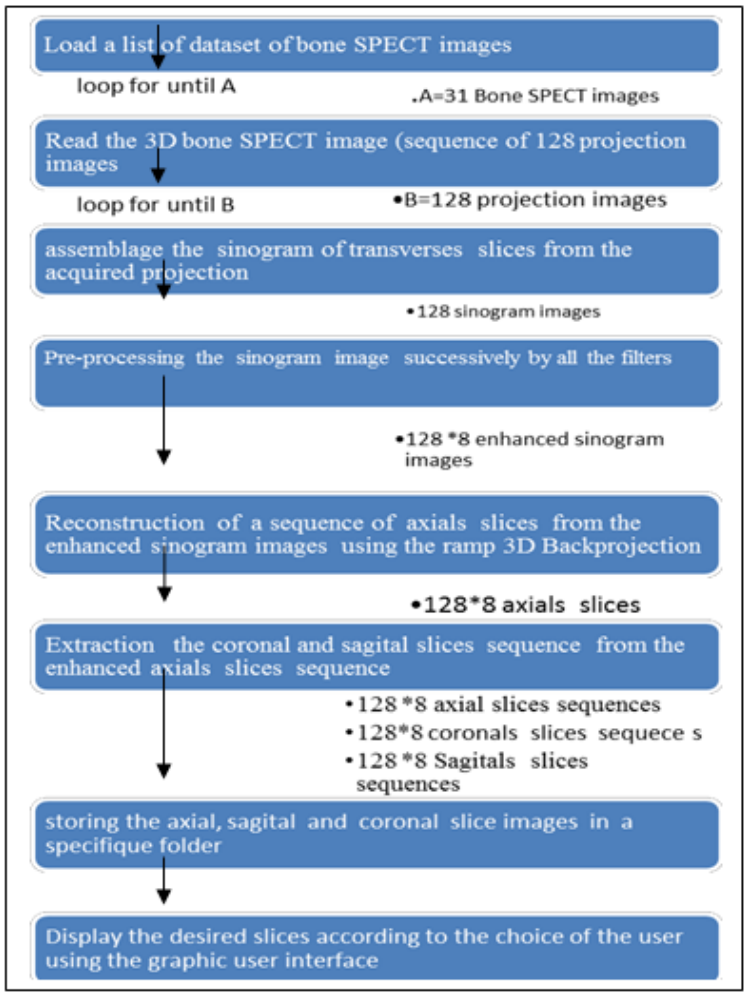

Figure 1

Proposed algorithm

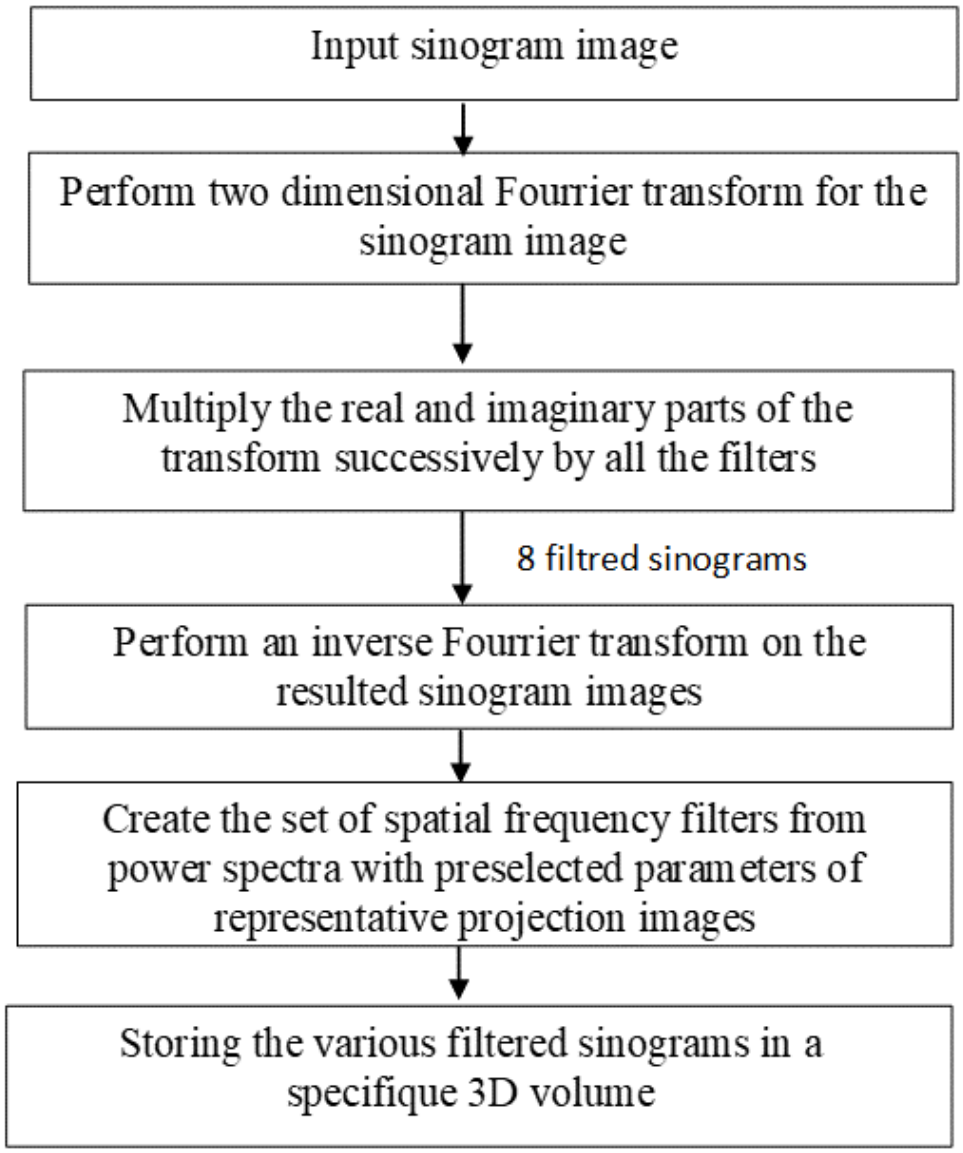

Figure 2

Block diagram of SPECT preprocessing method

```
. Image3d= back projection (3D data, theta, nx, ny,
          ps,dimx, dimy).
% Create the volume of projection images data3d =
  image2matrice3d( data3d );%u v k
%Define the dimension of the image geometry
%Define the dimension of the detector geometry
%Create the detector volume [my,mk,mu] =
   meshgrid (y,k,u);
% Create the original image volume
   [mx,my,mz] = meshgrid(x,y,z);
% Create a 'zero' volume (res3d)
res3d = zeros(nx,ny,nz);
% Create the 3d axial slices matrix For
t=1: number of projection angle
%Create the rotated coordinates (Mxu,Myy)of a back
projection plane using the Radon transform inverse
equation.
    Mxy=mx.*cos(thetas_rad(t))+my.*sin thetas_rad(t));
    Myk=mx.*sin(thetas_rad(t))+my.*cos (thetas_rad(t));
%Define the correspondent 2D sonogram
      sino2d = data3d(:,:,t);
%Produces a 3D sinogram copies of the 2D sonogram
     sino3d = repmat(sino2d, [1 1 nk]);
% A 3D sinogram interpolation is created using the results
of the Radon transform inverse to obtain the transverse
slices.
sino3d = interp3 (my,mk,mu, sino3d,mxy,myk,mz);
%reconstruct a 3D volume of the resulted 2 transverse
slices
    res3d = res3d + permute(sino3d,[2 1 3]); End
%Get the XYZ coordinates of the original density of
activity
. res3d = matrice2image3d (res3d);
.Image3d = fltr3D (res3d,'ramlak', 1)
 .End
```

Figure 3

Ramp 3D Back projection Reconstruction Where nx and ny are respectively the length and the width of the 3D volume of sinogram, ps is a depth- dependent point spread function, dimx and dimy are the dimensions of the 3D volume of the projections.

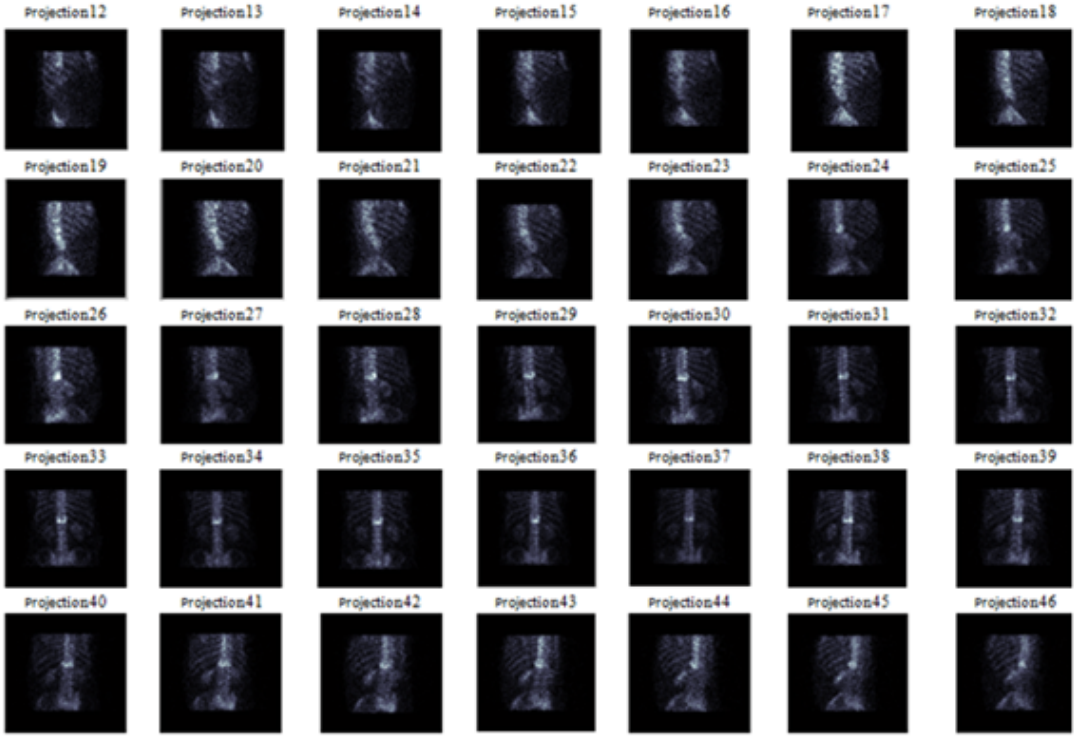

Figure 4

Input bone SPECT image, sequence of 128 projections, Displayed from right (projection12), to left (projection46).

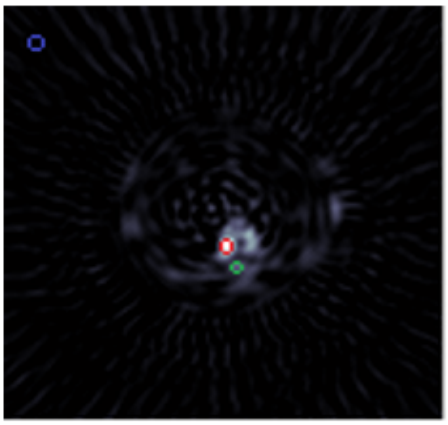

Figure 5

The measurements of maximum count in normal region of bone (Nmax(Normal)) (green outline), miximum count in hyperfuctionning bone (Nmax (abnormal)) (red outline),minimum count in background or bone hole region (Nmin (background)) (blue outline) for transverse slice filtered by Butterworth filter(fc=0.4,order=4).

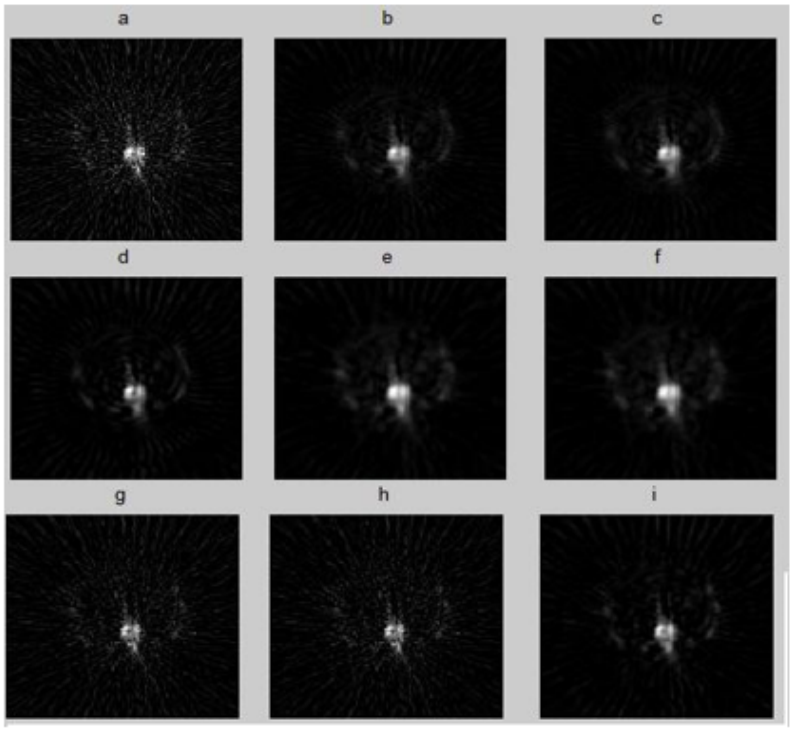

Figure 6

Transverse slice filtred with the best parameter of each filter: Ram- Lak, Hann, Hamming, Butterworth, Wiener, Metz, Parzen, Shepp-logan, Butterworth +Gaussian filter. a: simple retro projected with Ram-Lak filter. b: Hanning (cutoff =0.33) + Ramp filter (cutoff =1) c:Hamming (cutoff =0.3) + Ramp filter (cutoff =1) d: Butterworth(cutoff = 0.57, order = 9) + Ramp filter(cutoff =1) e: Wiener (FWHM = 7.8) + Ramp filter (cutoff =1) f: Metz (FWHM = 7.8) + Ramp filter (cutoff =1) g: Parzen (cutoff =0.5) + Ramp filter (cutoff =1) h: Shepp-logan (cutoff =0.35) + Ramp filter (cutoff =1) i: Gaussian (std=0.3)+butterworth (order=3, cutoff=0.47)+Ramp filter (cutoff =1),

Figure 7

Shepp-Logan phantom (Projection 64)

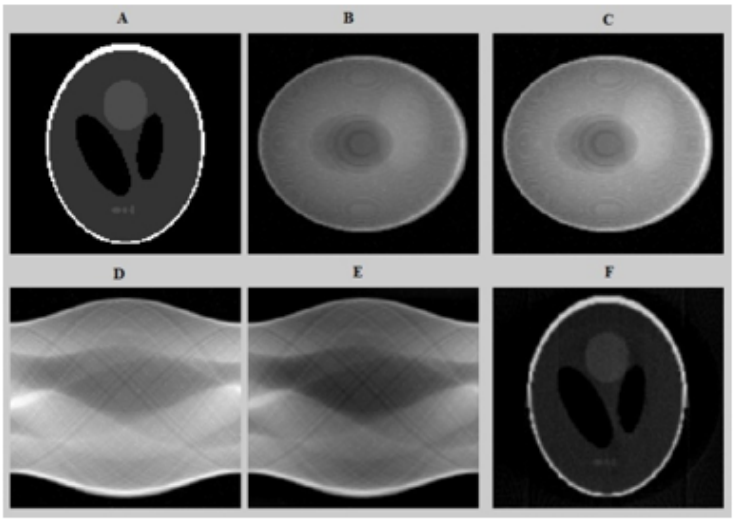

Figure 8

The different results of the proposed method.

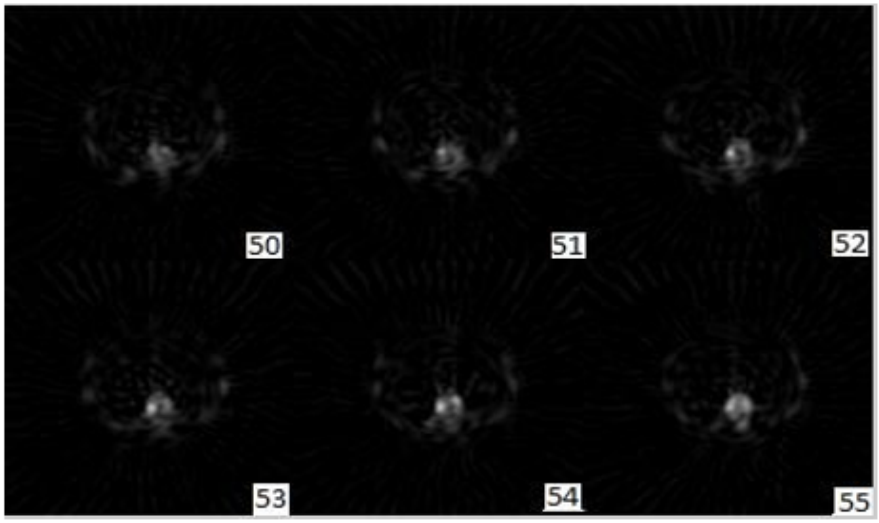

Figure 9

Output reconstructed transaxial slice with 1-pixel thick slice, displayed from cranial (slice50) to caudal (slice55).

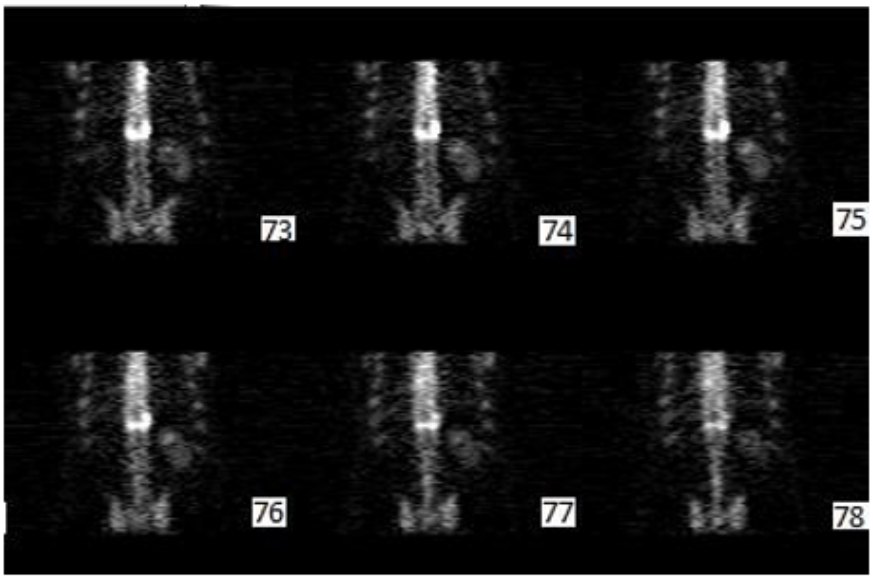

Figure 10

Output Coronal slices reconstructed from transaxial slice data with 1pixel thick slice. Displayed from posterior (slice73) to anterior (slice78).

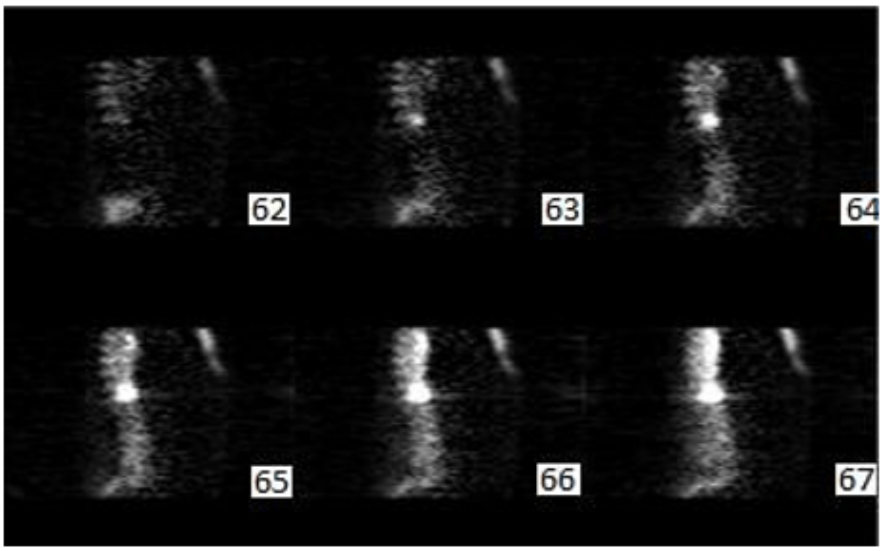

Figure 11

Output Sagittal slices reconstructed from transaxial slice data with 1pixels thick. Displayed from right (slice62), to left (slice67).

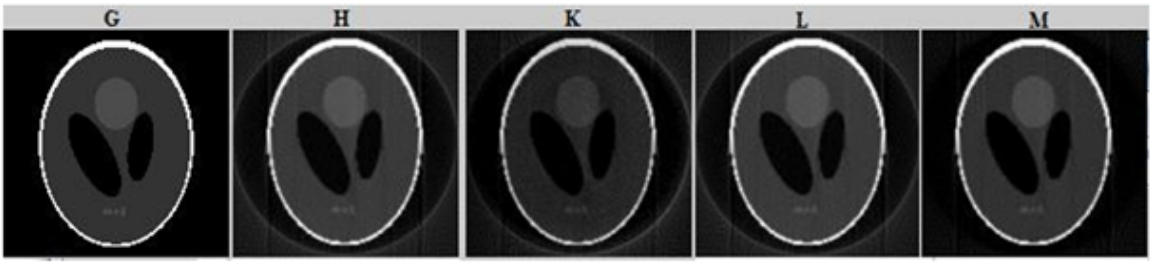

Figure 12

Shepp-Logan phantom image reconstructed from noisy projection including 6% Poisson noise distributed background events using different methods: the first row from the left column to the right are respectively:(G) the original Shepp-Logan phantom image (projection 64), (H) 3DFBP based on Gaussian filter combined with butterworth filter, (K) 3DFBP based on Gaussian filter, (L) 3DFBP based on Butterworth filter, (M) 3D FBP based on Gaussian filter combined with butterworth filter.

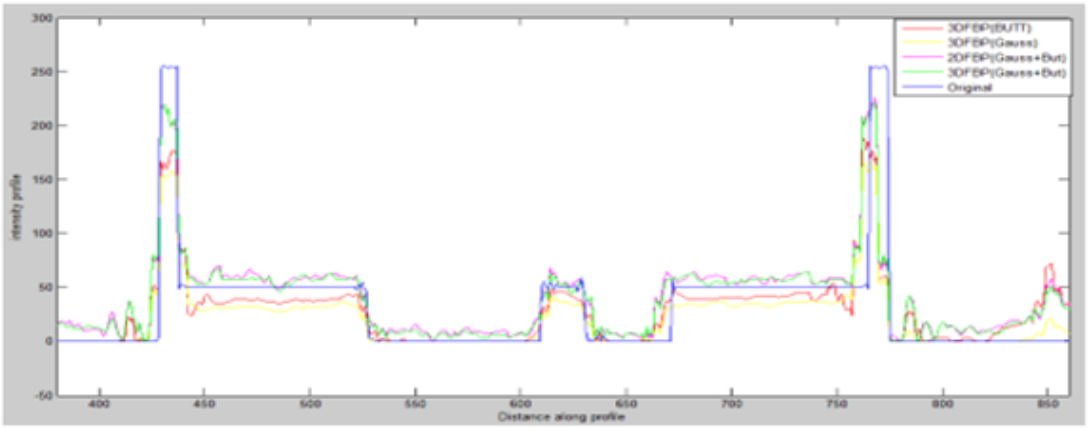

Figure 13

Line profile at row 81 of the noisy projection reconstructed respectively by: 2DFBP based on Gaussian filter combined with Butterworth filter, 3DFBP based on Gaussian filter, 3DFBP based on Butterworth filter and Proposed method, applied on noiseless projection.

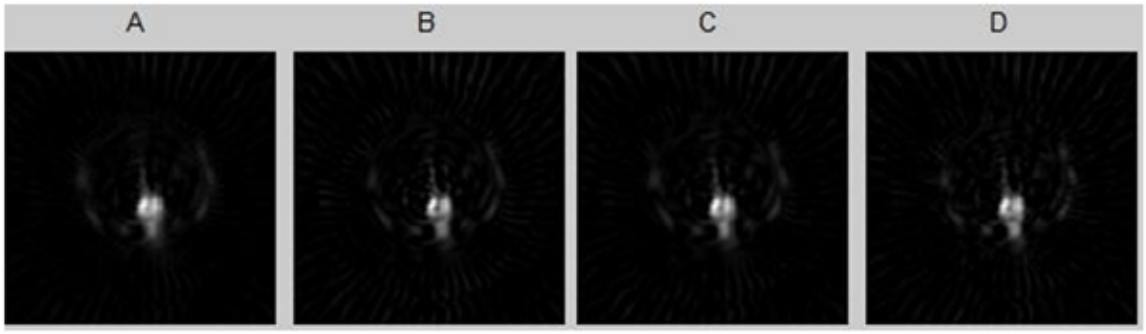

Figure 14

Transverse slices reconstructed respectively by: A. 3D FBP based on Gaussian filter, B. 3D FBP based on Butterworth filter, C. 2D FBP based on Gaussian filter combined with Butterworth, D. 3D FBP based on Gaussian filter combined with a Butterworth filter using the best parameters.

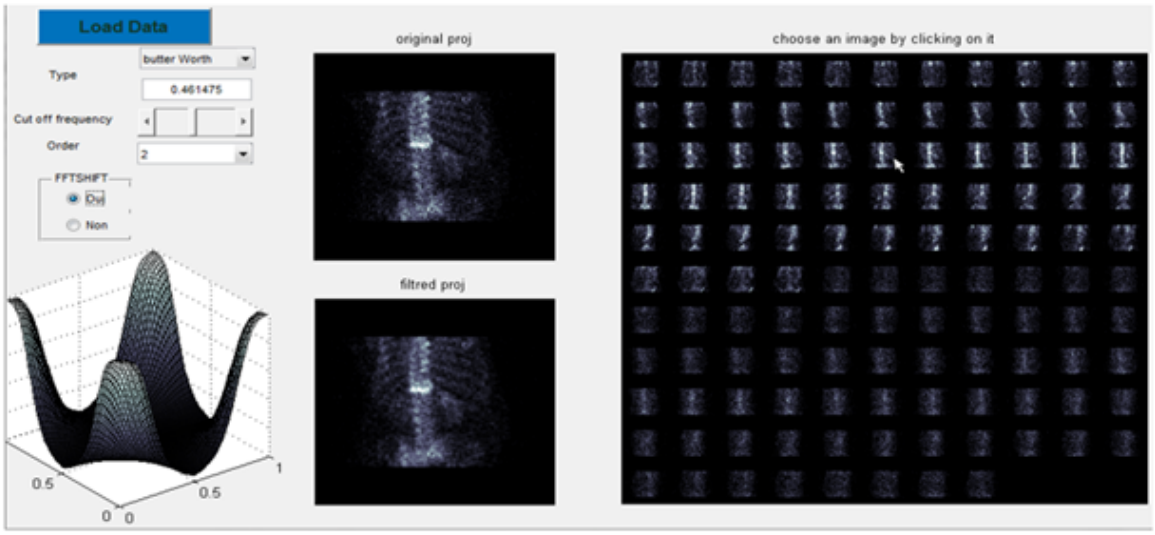

Figure 15

User graphical interface of SPECT Image denoising

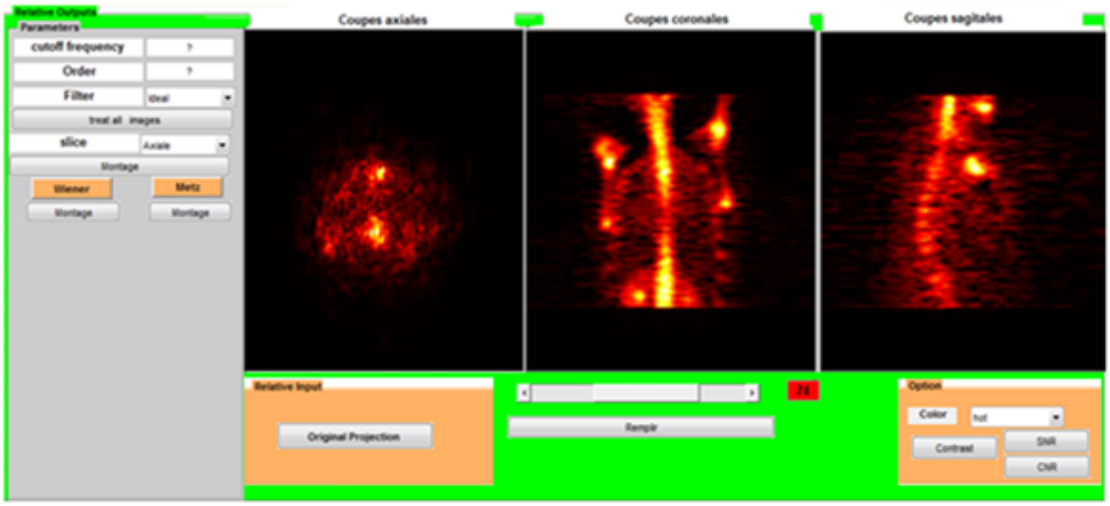

Figure 16

User graphical interface of SPECT Image reconstruction

Supplementary Files

This is a list of supplementary files associated with this preprint. Click to download.

- GraphicalAbstract.docx